EstProc

The development of new algorithms to parametise the mass settling flux of flocculated estuarine sediments

Produced within Defra Project FD1905 (EstProc)

AJ Manning

Report TR 145
Rev 2.0
November 2004

HR Wallingford

Document Information

Project	EstProc
Report title	The development of new algorithms to parametise the mass settling flux of flocculated estuarine sediments
Client	Defra
Client Representative	Jonathan Rogers
Project No.	CBS0022
Report No.	TR 145
Doc. ref.	Edited_TR145_rev2-0.doc
Project Manager	Richard Whitehouse
Project Sponsor	Richard Soulsby

Document History

Date	Revision	Prepared	Approved	Authorised	Notes
30/11/04	2.0	AJM	JS	RJSW	Final
20/08/04	1.0	AJM			Draft for review

Prepared ____________________

Approved ____________________

Authorised ____________________

Summary

EstProc

The development of new algorithms to parametise the mass settling flux of flocculated estuarine sediments

AJ Manning

Report TR 145
November 2004

IntroductionThe effective management of estuarine locations requires accurate models of fine sediment dynamics. For predicting the transport and fate of sediment movement in these situations, the determination of the various spatial and temporal mass fluxes is essential. One particular area which has caused numerous problems, is the modelling and mathematical description of the vertical mass settling flux of fine cohesive sediment, which becomes the depositional flux close to slack water. This flux is the product of the suspended particulate matter (SPM) concentration and the settling velocity. For non-cohesive sediment this is a relatively simple process as the settling velocity is proportional to the particle size. Whereas estuarine muds, which are composed of combinations of clay minerals and different types of biological matter, have the potential to flocculate in to larger aggregates called flocs.

The generality in application of existing floc parameterisation techniques specifically for mass settling flux determination, is a point of extreme debate and conjecture. It is therefore the aim of this study to describe a new flocculation model, developed as part of the UK Defra and EA funded EstProc research project (HR Wallingford, 2002), which was based entirely on experimental observations made using low intrusive data acquisition techniques, from a wide range of estuarine water column conditions. The empirical model will be used to reveal the principle inter-relationships controlling natural mud flocculation, and how this consequently effects the resultant depositional fluxes. The empirical model will then be assessed and compared against other approaches which are often incorporated in numerical sediment transport simulation models to parameterise the vertical mass flux.

Methodology
For the purpose of this study, it was the intention to generate statistical relationships from experimental data, and compare them with existing theoretical and empirical models. This empirical approach would allow the development of depositional algorithms which could easily be incorporated into numerical simulation models without the addition of a high volume of complex coding.

The database utilised in this study was acquired predominantly from a series of *in-situ* experiments conducted in several European estuaries. The majority of the floc sampling was made in the Tamar estuary (UK) as part of the European Commission MAST III funded COSINUS project. Additional *in-situ* floc samples were obtained from deployments conducted in both the Gironde (France) and Dollard (The Netherlands) estuaries. Sampling deployments were conducted on a sub-tidal cycle time scale at periods when the flow conditions were either reasonably steady or gradually changing. Supplementary flocculation data was provided from a

Summary continued

series of controlled hydraulic laboratory simulations conducted at the Laboratoire des Ecoulements Geophysiques et Industriels (LEGI) in Grenoble, France.

Flocs populations were sampled using the unique low intrusive INSSEV: *IN-Situ* SEttling Velocity instrument, which was developed at the University of Plymouth. Corresponding high frequency flow velocity and SPM concentration time series data were gathered using four two-channel 2 cm diameter discoidal electro-magnetic current meters (EMCM) and eight optical backscatter sensors. This collectively is referred to as the POST: Profile Of Sediment Transport system, and the various sensors were mounted on a vertical pole (attached to the bed frame) which was laterally off-set from the INSSEV sampling unit.

A parametric multiple regression statistical technique was chosen to analyse the empirical data matrix. The statistical package *Minitab for Windows - version 10.1* was used for all the regression analysis, with a default statistical confidence level of 95%. The aim was to separate the field of varying SPM concentration and shear stress empirical results, by curves representative of a number of parameter ranges.

Conclusion
This study has identified the key components which best quantitatively describe a floc population are: the changes in the macrofloc and microfloc settling velocities ($Ws_{macroEM}$ and $Ws_{microEM}$), together with how the suspended matter is distributed in each floc sub-population ($SPM_{ratioEM}$).

The importance of both turbulent shear stress and SPM concentration terms, as independent variables in controlling $Ws_{macroEM}$, was confirmed by a parametric multiple regression statistical analysis of empirical data which produced a highly significant R^2 of 0.91. The $Ws_{macroEM}$ algorithm (equation 14) displays a similar relationship to that proposed by Dyer (1989), with an increase in settling velocity at low shear stresses due to flocculation enhanced by shear, and floc disruption at higher stresses for the same concentration; the transition being a turbulent shear stress of about 0.36 N m^{-2}. This shear threshold corresponds very closely to the value observed during a series of laboratory annular flume experiments by Manning and Dyer (1999).

The combination of the three empirical algorithms into a single equation (18) to predict MSF, estimated the total MSF of the 157 measured floc samples from neap and spring tide conditions with a cumulative error of less than 4%. In comparison, the use of single settling velocity values of 0.5 mm s^{-1} and 5 mm s^{-1} were both in error by an average of -86% and +41%, respectively. Representing mean floc settling velocity by: *i)* a simple SPM concentration power-regression relationship, *ii)* the Lick *et al* (1993), and *iii)* the van Leussen (1994) approaches, all under predicted the total cumulative MSF by ~35-43%. Further analysis indicated that methods *M3-M10* all incurred high predictive errors (at times under-estimating by over 70%) as turbidity levels rose in close proximity to the bed. The Ws_{meanEM} (*M2*) proved to be the second most reliable method, although the errors in MSF prediction ranged from cumulative under-estimates of 14-25%.

The findings of this study demonstrate the empirical model (*M1*) has extreme flexibility in adapting to a wide range of estuarine environmental conditions, specifically for applied modelling purposes, by producing reliable mass settling flux predictions in both quiescent waters and the rare occurrence of very turbulent events experienced during extremely high flow velocity conditions where near-bed shear stresses could potentially reach 1-10 N m^{-2}. The *M1*

Summary continued

derived mass flux values were also valid for both water columns of very low turbidity and highly saturated benthic suspension layers with SPM concentrations approaching 8.6 g l^{-1}.

An algorithm has been devised (see Appendix 1) showing how the newly developed settling flux parameterisation can be implemented in computational sediment transport models.

Contents

Title page *i*
Document Information *ii*
Summary *iii*
Contents *vii*

1. Introduction to parameterising flocculation 1

2. Review of relevant flocculation literature 3
   2.1 Introduction 3
   2.2 Flocculation process 3
   2.3 Flocculation parameterisation 3

3. Methodology 6
   3.1 Introduction 6
   3.2 Data sources 6
   3.3 Data acquisition 6
      3.3.1 INSSEV floc population data 6
      1.1.2 POST hydrodynamic data 7

4. Data processing 8
   4.1 Introduction 8
   4.2 Floc data 8
   1.3 Turbulence data 9
   1.4 Multiple regression analysis 9

5. Results 12
   5.1 Introduction 12
   1.2 Macrofloc settling velocity ($Ws_{macroEM}$) 12
   1.3 Microflocs settling velocity ($Ws_{microEM}$) 13
   1.4 SPM ratio ($SPM_{ratioEM}$) 14
   1.5 Mass settling flux empirical model 15

6. Assessment of empirical settling flux model 16
   6.1 Introduction 16
   1.2 Comparison with measured fluxes 16
   1.3 Results of model inter-comparison 17

7. Summary and Conclusions 19

8. Acknowledgements 21

9. References 22

Tables

Table 1 Summary of floc parameterisation approaches used during the testing of the new empirical flocculation model (*M1*) 16
Table 2 Summary of the statistical output from each of the ten approaches mass settling flux predictions in comparison to the observed values. Negative percentage values indicate an under-estimate in the MSF prediction 17

Contents continued

Figures

Figure 1 Conceptual diagram showing the relationship between floc modal diameter, suspended sediment concentration and shear stress (Dyer, 1989)
Figure 2 INSSEV and POST sensors mounted on the estuarine bed frame – (*a*) front view and (*b*) side view
Figure 3 Representative plots of the statistically generated regression curves, together with the experimental data points, illustrating the three contributing components for the empirical flocculation model: *a*) Wsmacro EM (eqn 14), *b*) Wsmicro EM (eqn 15) and *c*) SPMratio EM (eqn 17)
Figure 4 The 157 individual mass settling flux (MSF) observations plotted against the corresponding 157 MSF values as predicted by each floc model approach (*M1-M10)*
Figure 5 The mean error (expressed as a %) demonstrated by each of the individual MSF values as calculated by each modelling method, for: *a*. all 157 flux values, *b*. Neap tides (112 flux values), and *c*. Spring tides (45 flux values). Negative values indicate overall errors which are under-predictions in MSF.
Figure 6 The cummulative total mass settling flux (MSF) expressed as a percentage, as calculated by each modelling method, for: *a*. all 157 flux values, *b*. Neap tides (112 flux values), and *c*. Spring tides (45 flux values). 100% = the total MSF observed
Figure 7 Individual mass settling flux (MSF) values, as predicted by each floc model approach (*M1-M10)* plotted against SPM concentration; for (*a*) 112 neap tide data points and (*b*) 45 spring tide data points. Each corresponding observed flux value is equal to 100%

Appendix

Appendix 1 Method Algorithm

1. Introduction to parameterising flocculation

The effective management of estuarine locations requires accurate models of fine sediment dynamics. For predicting the transport and fate of sediment movement in these situations, the determination of the various spatial and temporal mass fluxes is essential. One particular area which has caused numerous problems, is the modelling and mathematical description of the vertical mass settling flux of fine cohesive sediment, which becomes the depositional flux close to slack water. This flux is the product of the suspended particulate matter (SPM) concentration and the settling velocity. For non-cohesive sediment this is a relatively simple process as the settling velocity is proportional to the particle size. Whereas estuarine muds, which are composed of combinations of clay minerals and different types of biological matter, have the potential to flocculate in to larger aggregates called flocs.

Measurements of floc fall rates are a prerequisite for sediment transport models and early attempts to accurately measure floc settling velocities *in-situ* with devices such as Owen tubes (Owen, 1976) were not wholly successful, but were better than the laboratory derived data. Studies devoted to laboratory based analysis, were at variance with the Owen tube measurements, being lower in settling velocity. Optical devices to measure concentration profiles by Spinrad *et al* (1989), Kineke *et al* (1989), and McCave and Gross (1991) have sought to quantify the rate of water clearance, but they are unable, like all earlier instrumentation, to measure particle size and settling velocity spectra directly. Also, most of these systems can not claim to be obtaining their data from undisturbed *in-situ* conditions.

The recent advent of low intrusive *in-situ* floc sampling devices, in particular the INSSEV instrument (Fennessy *et al*, 1994), has provided a tool with which floc size and settling velocities can be measured simultaneously within a naturally turbulent flow, whilst creating minimal aggregate disturbance. This type of sampling device can provide an insight into the interaction of flocs with both turbulent eddies and SPM concentration during a tidal cycle, particularly within the lower layers of the flow where the turbulent shearing is greatest. Such site-specific information of floc settling velocity spectra is a prerequisite for accurate physical process parameterisation for the implementation into modelling applications.

Additionally, in contrast to laser diffraction particle sizers, only video-based sampling instruments which provide measurements of both floc size and settling velocity, can enable reliable estimates of floc effective density to be made by using a modified Stokes' Law. A knowledge of effective density is important in the calculation of vertical settling fluxes. As flocs increase in diameter they become more porous (> 90-95%); since the voids are filled with interstitial water; the higher order flocs are less dense than the lower order microflocs. Very few direct quantitative studies have been conducted on floc effective density variations. Floc fragility has precluded the direct measurement of floc density. Also the rheological properties of suspended particulate matter are governed by volume concentrations, as opposed to mass concentrations (Dyer, 1989).

The generality in application of existing floc parameterisation techniques specifically for mass settling flux determination, is a point of extreme debate and conjecture. It is therefore the aim of this paper to describe a new flocculation model, developed as part of the UK Defra and EA funded EstProc research project (HR Wallingford, 2002), which was based entirely on experimental observations made using low intrusive data acquisition techniques, from a wide range of estuarine water column conditions. The empirical model will be used to reveal the principle inter-relationships controlling natural mud flocculation, and how this consequently effects the resultant depositional fluxes. The empirical model will then be assessed and compared against other approaches which are often incorporated in numerical sediment transport simulation models to parameterise the vertical mass flux.

2. Review of relevant flocculation literature

2.1 INTRODUCTION

The complex ways in which cohesive sediments interact with continually varying hydrodynamic conditions are primary reasons for the current poor level of predictability of sediment movement within estuarine locations. Therefore section 2.2 summaries the key aspects of mud flocculation in turbulent estuarine flows. Whilst section 2.3 provides a review of the floc parameterisation approaches which are most commonly used in predictive sediment transport model.

2.2 FLOCCULATION PROCESS

The rate of flocculation is a function of: sediment particle concentration, salinity, mineralogy, bio-chemical composition of the suspended matter, and the physical mechanisms which bring the cohesive particles into contact (Manning, 2004a). Van Leussen (1988) theoretically assessed the comparative influence of the three main collision mechanisms: Brownian motion, turbulent shear and differential settling, and deduced that turbulent shear stresses, principally those generated by velocity gradients present in an estuarine water column, were the dominant flocculation mechanism. This mechanism was deemed most effective for turbulent shear values of 1-10 s^{-1} (0.5 m above the bed) which corresponds to turbulent shear stresses ranging between 0.03-0.8 N m^{-2}. These turbulent shear rates are representative of those typically experienced in the near bed region of many European macrotidal and mesotidal estuaries.

The efficiency with which the particles coagulate is a reflection of the stability of the suspension (van Leussen, 1994). A suspension is classified as unstable when it becomes fully flocculated, and is stable when all particles remain as individual entities. The statistical occurrence of collisions further increases as the abundance of particles in suspension rise. Although turbulent shear can promote floc growth, high levels of turbulence which occur during a tidal cycle, can in turn cause disruption to the flocculation process by instigating floc break-up, and eventually pull the constituent components of a floc apart. McCave (1984) advocated that turbulence determines the maximum floc size in tidal waters. The energy for turbulent mixing is derived from the kinetic energy dissipated by the water flowing across a rigid rough boundary. The frictional force exerted by the flow per unit area of the bed is the shear stress (turbulent shear stress during turbulent flow conditions). As turbulent activity increases - both turbulent pressure differences and turbulent shear stresses in the flow rise. If the floc structural integrity is less than the imposing turbulent induced forces, the floc will fracture. Also, aggregate break-up can occur as a result of high impact particle collisions during very turbulent episodes. Floc break-up by three-particle collisions tends to be the most effective (Burban *et al,* 1989). Hence, turbulent shear stress can impose a maximum floc size restriction on the floc population. Eisma (1986) observed a general agreement between the maximum floc size and the smallest turbulent eddies as categorised by Kolmogorov.

2.3 FLOCCULATION PARAMETERISATION

The specification of the flocculation term within numerical models depends upon the sophistication of the model. The most simplistic parameterisation is a settling velocity value which remains constant in both time and space. These fixed settling values are typically selected on an arbitrary basis and adjusted by model calibration. The next step has been to use data provided by field settling tube experiments to relate flocculation to SPM concentration. Empirical results have shown a general exponential relationship between median floc settling velocity (Ws_{50}) and SPM for concentrations ranging up to 10 gl^{-1}. However, both of these parameterisation techniques do not include the important influential effects of turbulence.

More recently, a number of authors have proposed simple theoretical formulae inter-relating a number of floc characteristics which can then be calibrated by empirical study. Such an approach has been used by van Leussen (1994), who has utilised a formula which modifies the settling velocity in still water, by a growth factor due to turbulence and then divided by a turbulent disruption factor:

$$Ws = W_{so}\left(\frac{1+aG}{1+bG^2}\right) \tag{1}$$

where Ws is the floc settling velocity, G is the root mean square of the gradient in turbulent velocity fluctuations, a and b are empirically determined constants. G (with the units s^{-1}) is obtained by taking the square root of the turbulent energy dissipation rate ε divided by the kinematic viscosity ν.

$$G = \left(\frac{\varepsilon}{\nu}\right)^{0.5} \tag{2}$$

The reference settling velocity (taken at zero turbulent conditions), W_{so}, is then related to the SPM concentration (C) by:

$$W_{so} = k \cdot C^m \tag{3}$$

where k and m are empirical constants. Equation 1 is a qualitative simplification of an Argaman and Kaufman (1970) model originally developed for the sanitation industry, with only a limited number of inter-related parameters, and hence does not provide a complete description of floc characteristics within a particular shear environment.

A number of authors have attempted to observe how the floc diameter changes in turbulent environments. In particular, Lick *et al* (1993) derived an empirical relationship based on laboratory measurements made in a flocculator. They found the floc diameter (D) varied as a function of the product of the SPM concentration (C) and the turbulence parameter G:

$$D = c(C \cdot G)^{-d} \tag{4}$$

where c and d are empirically determined values. However, this formulation tells you very little about the important floc settling or dry mass properties.

An approach which has recently gained much interest by numerical modellers, is the fractal representation of flocs (e.g. Winterwerp, 1999). Fractal theory is dependent on the successive aggregation of self-similar flocs producing a structure that is independent of the scale considered. This is similar to Krone's (1963) order of aggregation. Winterwerp (1998) obtained the following relationship (based on research by

Kranenburg, 1994) relating floc settling (Ws) to the: floc size (D), primary particle diameter (D_p) and the fractal dimension (nf):

$$W_S = \alpha' D_p^{3-nf} [(\rho_{sed} - \rho_w) g] / \mu D^{nf-1} \quad (5)$$

where: α' is an empirically derived constant, ρ_{sed} and ρ_w the sediment and water density respectively, μ is the dynamic molecular viscosity of water and g is gravity. Values for the fractal dimension generally range between 1 and 3; 1-1.4 representative of fragile aggregates and 2.5-3 representative of more strongly bonded estuarine flocs. This allows corresponding settling velocity values to be estimated from measurements of floc size, such as those made by a laser particle sizer. However, in order to make a fractal based model solvable analytically within a numerical sediment transport simulation, a mean nf of 2 is commonly assumed.

However, apart from the general fact that suspended particulate matter flocculates and flocculation typically dominates over break-up, at present it has not been possible to quantify the influence and occurrence of flocculation, as well as floc break-up, on *in-situ* estuarine floc distributions. Although a conceptual model illustrating probable trends was proposed by Dyer (1989, Figure 1), relatively little quantitative empirical data has been obtained to test potential hypotheses and quantify floc-turbulence inter-relationships. This is mainly due to the fragility of the fastest settling macroflocs, which are easily broken-up upon sampling. The presence of large estuarine macroflocs was observed *in-situ* by both underwater photography (Eisma *et al*, 1990), and measurements provided by laser particle sizers (Bale and Morris, 1987). Stokes' Law has been commonly used to estimate the settling velocity of laser diffraction particle sizer measurements. This requires making an assumption of the floc density. The most practical density value in relation to mud flocs, is that of effective density, ρ_e (also known as density contrast, density difference or excess density). Effective density is the floc bulk density (ρ_f) less the density of the interstitial water (i.e. $\rho_e = \rho_f - \rho_w$). However, the settling velocity of a floc is the function of both its floc size and effective density, and all three of these floc components can display variations spanning three to four orders of magnitude within any one floc population (Lick, 1994; Fennessy and Dyer, 1996; Manning, 2001; ten Brinke, 1994).

3. Methodology

3.1 INTRODUCTION

The method proposed is essentially to derive quantifying relationships using statistical analysis of a unique comprehensive database of flocculation properties and turbulence characteristics. Section 3.2 outlines the scope of the database, and section 3.3 describes the relevant data acquisition techniques.

3.2 DATA SOURCES

The data utilised in this study was acquired predominantly from a series of *in-situ* experiments conducted in several European estuaries. The majority of the floc sampling was made in the Tamar estuary (UK) as part of the European Commission MAST III funded COSINUS project. A series of four Tamar estuary experiments provided a total of 91 floc populations (i.e. complete spectral samples) which were measured during neap and spring tidal conditions (Dyer *et al*, 2002; Manning and Dyer, 2002a). An additional 45 *in-situ* floc samples were obtained from deployments conducted in both the Gironde (France) and Dollard (The Netherlands) estuaries. The Gironde estuary is macrotidal and predominantly well mixed. The 34 floc measurements (Manning *et al*, 2004) acquired during the EC TMR SWAMIEE project, were made during neap tidal conditions in the lower reaches of the Gironde estuary, near Le Verdon. Within the framework of the EC MAST III INTRMUD project (Dyer *et al*, 2000), the 11 measurements were made during neap tides in the mesotidal Dollard estuary. In contrast to the Tamar and Gironde *in-situ* experiments, the instrumentation was deployed on intertidal mudflats. Particulate entrainment and turbulence levels were similar to those observed during neap tides in the Tamar estuary. Sampling deployments were conducted on a sub-tidal cycle time scale at periods when the flow conditions were either reasonably steady or gradually changing. Supplementary flocculation data was provided from a series of controlled hydraulic laboratory simulations (Gratiot and Manning, 2004) conducted at the Laboratoire des Ecoulements Geophysiques et Industriels (LEGI) in Grenoble, France.

3.3 DATA ACQUISITION

3.3.1 INSSEV floc population data

Flocs were sampled using the low intrusive INSSEV: *IN-Situ* SEttling Velocity instrument, which was developed at the University of Plymouth (Fennessy *et al*, 1994). The sampling apparatus comprises a twin chamber device, where by a volume of estuarine water is captured in the upper chamber (Figure 2). After a period of 10-20 s had elapsed (to allow the turbulence in the water to decay), a selection of flocs were permitted to pass into a lower settling column through a computer controlled trap door. An integral underwater back-lit video camera viewed the flocs as they settle within the lower settling chamber. The floc images were recorded using an S-VHS video suite, which had a practical lower size detection limit of 20 μm. The INSSEV device has the distinct advantage of permitting the simultaneous *in-situ* measurement of both individual floc size, and settling velocity from which the floc effective density can be calculated. A detailed review of the INSSEV instrument and its operation is provided by Manning and Dyer (2002b). During a sampling run, complete floc population samples were acquired at a rate of one sample every 10-20 minutes; the interval being dependent upon the floc settling velocities and SPM concentration. The INSSEV apparatus was mounted on a metal frame, with floc measurements made at a nominal height of 0.5 m above the bed. This near-bed region typically contains approximately 80% of the turbulent energy present within an estuarine water column, which is significant for both floc formation and aggregate break-up, which can lead to continual particle recycling and re-entrainment.

3.3.2 POST hydrodynamic data

Corresponding high frequency flow velocity and SPM concentration time series data were gathered using four two-channel 2 cm diameter discoidal electro-magnetic current meters (EMCM) and eight optical backscatter (OBS) sensors. This collectively is referred to as the POST: Profile Of Sediment Transport system (Christie *et al*, 1997) and was also developed at the University of Plymouth. The various POST sensors were mounted on a vertical pole (attached to the bed frame) which was laterally off-set from the INSSEV sampling unit (Figure 2). All POST sensors, together with a Druck pressure transducer to measure changes in the water depth, recorded continuously at a rate of 18 Hz and were low pass filtered at 5 Hz to prevent aliasing. In order to quantify the turbulent fluctuations, EMCMs were arranged in pairs, to measure the three orthogonal components of the flow at both 25 cm and 75 cm above the bed. Laboratory calibration and zero offset checks suggest the accuracy of an EMCM was about ± 3%, but their digital resolution was approximately ± 0.6 mm s^{-1}. The OBSs were arranged approximately logarithmically through the bottom 1 m of the flow. Water samples were collected for OBS calibration, which was also to an accuracy of about ± 3%, although their resolution was of the order of ± 5 mg l^{-1}. The close proximity of the INSSEV instrument, and the turbulence and SPM concentration measurements, allows direct comparisons between the results. Through depth vertical profiles of temperature and salinity were taken at regular intervals by a Sea-Bird Electronics Seacat SBE 19-03 CTD.

4. Data *processing*

4.1 INTRODUCTION

This section initially outlines the processing computations which were applied to both the raw floc and turbulence data. This is followed by a description of the multiple parametric statistical analysis conducted on the resultant integrated data matrix.

4.2 FLOC DATA

Floc sizes were measured both along their axis in the direction of settling (D_Y), and their axis perpendicular to it (D_X). A spherical equivalent floc diameter, D, was then determined:

$$D = (Dx \cdot Dy)^{0.5} \quad (6)$$

The simultaneous measurement of floc size and settling velocity (W_S) allows the effective density (ρ_e) of individual flocs to be calculated from a re-arranged Stokes' Law relationship

$$\rho_e = (\rho_f - \rho_w) = \frac{Ws\ 18\mu}{D^2\ g} \quad (7)$$

where g is gravity, and μ is the dynamic molecular viscosity of water. Computational techniques outlined by Fennessy *et al* (1997) were then applied, for the calculation of individual floc dry mass and the mass settling flux (MSF) distribution for each INSSEV floc sample.

The arithmetic mean size is the most commonly used floc parameter. However, from a quantitative point of view, the large variations in floc density, size and settling velocity which are often apparent in any one sample tend to question the validity of a single mean value. For a more quantitative analysis, a better approximation is to segregate a complete floc population into two distinct floc size fractions: *macroflocs* and *microflocs*. The larger fraction are the macroflocs, and these tend to be fast settling aggregates which are typically the same diameter as the turbulent Kolmogorov microscale. Although floc density generally decreases as the macroflocs grow, their settling velocities increase quite significantly. These low densities indicate that the macroflocs could potentially progressively break down in regions of higher turbulent shear stress to form the component microflocs.

An appraisal of the data reported in this study by Manning (2001), revealed that 160 μm provided the optimum separation point between the macrofloc and microfloc fractions. Whereby the characteristics, in particular the settling velocity and dry mass, of each floc sub-population were consistently significantly different for a wide range of turbulent shear stresses and SPM conditions. Macrofloc characteristics for a sample were determined by calculating the dry mass weighted arithmetic mean, for each floc parameter, from the flocs which were greater than 160 μm in diameter. Microfloc properties were calculated for the sub-group $D < 160$ μm.

4.3 TURBULENCE DATA

The three orthogonal components of flow measured by the *in-situ* EMCMs enabled the turbulent shear stresses to be quantified, at the two heights, from the turbulent kinetic energy (E) derived using the relationship:

$$E = 0.5\ \rho_W\ \left(\overline{u'^2} + \overline{v'^2} + \overline{w'^2}\right) \tag{8}$$

where $\overline{u'^2}$, $\overline{v'^2}$ and $\overline{w'^2}$ are the variances of the three turbulent fluctuating components calculated from each 3 minute 47.55 second duration file. The value of E was relatively insensitive to the orientation of the EM's, when compared to the logarithmic profile or Reynolds stress approaches (Heathershaw, 1979). Assuming the energy production equals the energy dissipation (Nakagawa and Nezu, 1975), the turbulent shear stress (τ) was calculated from E by:

$$\tau = 0.19 \cdot E \tag{9}$$

The constant of proportionality in equation 9 applies to wide variety of flows (Soulsby, 1983). For the laboratory grid tank measurements, the turbulent structure of the water column was quantified from the turbulent frictional velocity component, U_*, derived from high frequency acoustic Doppler velocimeter measurements. Values of τ are related to U_* and ρ_w by:

$$U_* = \left(\frac{\tau}{\rho_w}\right)^{0.5} \tag{10}$$

For comparative purposes, the turbulent structure of the water column could also be shown in terms of the root mean square of the gradient in the turbulent velocity fluctuations (G) with the units s^{-1}:

$$G = \left[\frac{U_*^3}{(\kappa \cdot \nu \cdot z)}\right]^{0.5} \tag{11}$$

where ν is the kinematic viscosity (molecular viscosity divided by the density of water), κ is the Von Karman constant and z is the distance above the estuary bed. A second comparative parameter is the Kolmogorov microscale (Kolmogorov, 1941a and b) eddy size. Kolmogorov classified turbulence levels by the size of the dissipating eddies, η (units are μm), in a turbulent flow and these can be calculated by equation 12:

$$\eta = \left(\frac{\nu}{G}\right)^{0.5} \tag{12}$$

4.4 MULTIPLE REGRESSION ANALYSIS

For the purpose of this study, it was the intention to generate statistical relationships from the experimental data, and compare them with existing theoretical and empirical models. This empirical approach would allow the development of depositional algorithms which could easily be incorporated into numerical simulation models without the addition of a high volume of complex coding.

A parametric multiple regression statistical technique was chosen to analyse the empirical data matrix. The statistical package *Minitab for Windows - version 10.1* was used for all the regression analysis, with a default statistical confidence level of 95%. The aim was to separate the field of varying SPM concentration and τ empirical results, by curves representative of a number of parameter ranges. A preliminary regression analysis of the macrofloc and microfloc parameters was undertaken for each of the data sets separated at 160 μm. Different combinations of independent and dependant variable were assessed, so as to reveal where the strongest inter-correlations existed.

The following floc characteristics were considered the most important and relevant (abbreviations used in brackets):

- Macrofloc settling velocity (Ws_{macro})
- Microfloc settling velocity (Ws_{micro})
- Percentage of SPM constituting the macrofloc portion of a floc population ($SPM\%_{macro}$)
- Percentage of SPM constituting the microfloc portion of a floc population ($SPM\%_{micro}$)
- Total SPM concentration (SPM)
- Turbulence parameters (τ or G).

The division of particulate matter within a floc population, and the relative rates at which they settle, are the key variables which govern the deposition of the matter in suspension; i.e. the mass settling flux, and these are represented by the first five terms. Also the physical descriptors of SPM concentration and a turbulence parameter, represent the basic factors which govern the collision rate and subsequent degree of flocculation of particles in estuarine waters. In this quantitative study salinity was not regarded as a prime factor in flocculation, as significant levels of flocculation were observed in the Tamar and Dollard when the water was predominantly fresh. Also, organic matter descriptors were omitted from the analysis, as there was only a limited number of bio-chemical samples available.

A key assumption used in the analysis was that there was no inclusion of an additional flocculation time (T_F) component (Winterwerp, 1999). For laboratory studies it is possible to allow the flocs to obtain equilibrium with the turbulent flow field as the duration of exposure to turbulent shearing can be controlled. Van Leussen (1994) stated T_F as the time needed to decrease the original number of individual unflocculated particles in a suspension, to 10% as a result of particle adheration through flocculation induced aggregate growth, and suggested that T_F could be estimated by:

$$T_F = \frac{2.306 \cdot \pi}{4 \cdot \alpha \cdot \phi (10 + G)} \tag{13}$$

where α is a cohesion collision efficiency factor, and ϕ is the total volume of sediment per unit volume. From Gibbs (1983) a nominal α value of 0.18 was estimated for Tamar, Gironde and Dollard estuary muds. The file length of 3 minute 47.55 second would be a valid T_F for a combined G value of 1 s^{-1} and SPM concentration of approximately 50 mg l^{-1} (i.e. the lowest collision rate attainable) to achieve flocculation equilibrium. For G and SPM concentrations above these values, floc equilibrium would theoretically occur within the duration of a file.

From examination of the various combinations of G and SPM from the entire data matrix, only 3% of the data points had a T_F exceeding the mean turbulent shear values file duration (i.e. 3 minute 47.55 seconds). This 3% represented flocs which were measured at quiescent periods during neap tides when most of the larger macroflocs had probably settled to the bed. This implies that the majority of the neap tide flocs and all of those observed during spring tides had attained equilibrium with the ambient estuarine conditions. If any of the 3% cluster registered as an "unusual observation" from the regression summary, it was rejected. Therefore, the assumption of full flocculation was considered justified for all the *in-situ* data used for the regression analysis.

For consistency, the following units were used for each parameter included in the multiple regression and comparison analysis: τ = N m^{-2}, G = s^{-1}, SPM = mg l^{-1}, Ws = mm s^{-1}, D = μm, and $SPM\%_{macro}$ and $SPM\%_{micro}$ = both expressed as a percentage. Note that the comparative G and Kolmogorov eddy size values stated in the analysis are determined at a height z = 50 cm above the estuary bed (i.e. nominal INSSEV sampling height), unless otherwise stated.

5. Results

5.1 INTRODUCTION

The regression analysis which produced the empirical model (denoted by the suffix $_{EM}$) for estuarine flocculation was based on a combined data matrix consisting of 157 individually observed floc populations. The derived algorithms are valid for SPM concentration and τ values ranging between 10-8600 mg l^{-1} and 0.04-2.13 N m^{-2} (with extrapolation extending this up to 10 N m^{-2}), respectively. This allows the empirical model to be more readily implemented into numerical simulation models of sediment transport. Therefore, this empirical model was composed of three principle component algorithms: $Ws_{macroEM}$, $Ws_{microEM}$ and $SPM_{ratioEM}$; each will be discussed in turn.

5.2 MACROFLOC SETTLING VELOCITY ($WS_{MACROEM}$)

Macroflocs (D > 160 μm) are recognised as the most important sub-group of flocs, as their fast settling velocities tend to have the most influence on the mass settling flux. Their fragile, low density structure makes them very sensitive to physical disruption during sampling. Consequently, most previous experimental studies have tended to emphasise and favour the smaller microflocs.

The multiple regression revealed that the $Ws_{macroEM}$ showed a dependency on both τ and SPM concentration variations. It was not possible for a single equation to encompass the entire experimental range of turbulent shear stress, and thus the data was split into three τ zones which could be joined at the boundaries.

For τ ranging between 0.04-0.7 N m^{-2}:

$$Ws_{macroEM} = 0.644 + 0.000471\ SPM + 9.36\ \tau - 13.1\ \tau^2 \qquad R^2 = 0.93 \tag{14a}$$

For τ ranging between 0.6-1.5 N m^{-2}:

$$Ws_{macroEM} = 3.96 + 0.000346\ SPM - 4.38\ \tau + 1.33\ \tau^2 \qquad R^2 = 0.90 \tag{14b}$$

For τ ranging between 1.4-5 N m^{-2}:

$$Ws_{macroEM} = 1.18 + 0.000302\ SPM - 0.491\ \tau + 0.057\ \tau^2 \qquad R^2 = 0.99 \tag{14c}$$

Continuity between each relationship can be achieved by calculating a $Ws_{macroEM}$ value using both adjacent equations (at a specific τ) and obtaining a single transitional $Ws_{macroEM}$ value from linear interpolation. The transition shear stress zones between equations 14a-14b and 14b-14c, are 0.6-0.7 N m^{-2} and 1.4-1.5 N m^{-2}, respectively. Each formulation is valid for concentration values up to 8.5 g l^{-1}. However, no data points were available for SPM concentrations over 1 g l^{-1} when the turbulent shear stress fell below 0.1 N m^{-2}, and therefore this should be regarded as a further boundary limit to equation 14a. The regression analysis indicated that the concentration contributed 66% of the total variance, whilst of the remaining 34% attributed to the turbulence parameters, approximately a third (of the 34%) is accredited to the τ^2 term.

The complete regression curves described by equations 14a-14c are represented graphically in Figure 3a. Generally, $Ws_{macroEM}$ displays a similar relationship to that proposed by Dyer (1989, see Figure 1), with an increase in settling velocity at low shear stresses due to flocculation enhanced by shear, and a decrease in settling velocity due to floc disruption at higher stresses for the same concentration. The limit being a turbulent shear stress of about 0.36 N m^{-2} (equivalent G = 5.67 s^{-1} and Kolmogorov microscale eddy size = 428 μm). This shear stress threshold corresponds very closely to the value observed during a series of laboratory annular flume experiments by Manning and Dyer (1999).

A number of authors have attributed the formation of very large flocs to differential settling, but if this mechanism was to be significant it would only be able to operate at low values of τ. The data points on Figure 3a, identify that SPM concentrations > 0.5 g l^{-1} were only present when the shear stress typically exceeded 0.12 N m^{-2}, so that differential settling would not be important in this case. The ineffectiveness of differential settling as a growth mechanism for natural estuarine flocs agrees with the findings of Stolzenbach and Elimelich (1994).

The peak macrofloc settling velocities (~4-6 mm s^{-1}) were representative of flocs which form within a CBS layer, where damping effects within the CBS reduces the magnitude of the turbulent stirring. At this point the collision frequency appeared to be at its optimum for flocculation and stimulated the growth of fast settling macroflocs. Above 0.4 N m^{-2}, the regression shows the $Ws_{macroEM}$ values decreased rapidly in response to disaggregation as the turbulent shear increased. For a sheared suspension of 4 g l^{-1}, a τ of 0.7 N m^{-2} led to a 33% decrease in $Ws_{macroEM}$. This must be the effect of the continued increase in shear creating more destructive collisions between the abundant macroflocs, and negating those causing flocculation. The decrease in settling velocity would therefore be attributed to a general reduction in the floc size range within the macrofloc sub-group.

Above a τ of 1.4 N m^{-2}, the $Ws_{macroEM}$ tended to decrease more slowly with increasing shear. One could hypothesise that beyond 1 N m^{-2}, only a limited number of very resilient macroflocs would exist, and further growth would be eradicated with a continued rise in shear stress. This small number of very strong macroflocs would have been created during very highly turbulent events, and retained that “history” as they become trapped in the estuary’s residual circulation and moved towards the estuary head.

For the very high shear stress region between 5-10 N m^{-2}, any further macrofloc settling velocity reduction would occur at an extremely slow rate with increasing turbulence. Therefore, for applied modelling purposes the $Ws_{macroEM}$ at a τ of 10 N m^{-2}, for a particular SPM, could be assumed to be equal to that value determined by equation 14c using a shear stress input of 5 N m^{-2}, without incurring any significant reduction in computational accuracy (on the rare occasion that such turbulent conditions would occur). In other words for applied modelling purposes, above a τ of about 5 N m^{-2}, the $Ws_{macroEM}$ can be considered to remain effectively constant.

5.3 MICROFLOCS SETTLING VELOCITY ($WS_{MICROEM}$)

The smaller microflocs (D < 160 μm) are generally considered to be the building blocks from which the macroflocs are composed. The microfloc class of aggregate tend to display a much wider range in effective densities and settling velocities than the larger floc fraction. The settling trends of the microflocs were represented by two sub-algorithms.

For τ ranging between 0.04-0.55 N m^{-2}:

$$Ws_{microEM} = 0.244 + 3.25\,\tau - 3.71\,\tau^2 \qquad R^2 = 0.75 \qquad (15a)$$

For τ ranging between 0.51-10 N m^{-2}:
$Ws_{microEM} = 0.65\ \tau^{-0.541}$ $R^2 = 0.73$ (15b)

A transition zone between equations 15a and 15b occurred between a τ of 0.51-0.55 N m^{-2}. A single $Ws_{microEM}$ value is obtained by linear interpolation between the two values calculated by both equations in this transitional shear zone. The most prominent difference to be revealed when comparing the $Ws_{macroEM}$ and $Ws_{microEM}$ algorithms, was the negligible influence of SPM concentration variations on the latter. The shape of the regression curve is illustrated graphically in Figure 3b, where it is plotted together with the corresponding data points.

$Ws_{microEM}$ demonstrated a correlation solely with turbulent shear stress. The lower R^2 values of algorithms 18a and 18b, when compared to those of the macrofloc settling velocity, was partly a result of the greater variability in the individual settling velocities and effective densities exhibited by the microfloc distributions, from which each of the average microfloc settling velocities was calculated. The scatter is a reflection of the greater variability in the settling and compositional properties exhibited by individual microflocs within a single floc population. This in turn would have an effect on each $Ws_{microEM}$ value calculated, however an R^2 of 0.73-0.75 suggests that the scatter is relatively small. Hence, these equations are deemed representative of the empirical data, for modelling applications.

As with the macroflocs, the microfloc settling velocity rose with increasing shear stress until a peak $Ws_{microEM}$ of ~1 mm s^{-1} was reached at a limiting τ of ~0.42 N m^{-2} (equivalent G = 6.43 s^{-1} and Kolmogorov microscale eddy size = 402 μm). This probably represents growth in the number of larger microflocs (D = 120-160 μm), by scavenging the very small microfloc sub-fractions (D < 80 μm) during conditions which were most conducive for flocculation. However, this growth was significantly slower than the comparative macroflocs.

It must be noted that if both equations 14 and 15 are to be incorporated into the framework of a numerical model where the turbulence input parameter is of the turbulent shear G format, all the τ functions must be replaced with the following τ_{mod} sub-equation, which is a modified rearrangement of equation 11:

$$\tau_{mod} = \rho_w \left[(G^2 \cdot \kappa \cdot \nu \cdot z)^{1/3}\right]^2 \quad (16)$$

This is because unlike the τ parameter used in the multi-regression analysis, corresponding values of G are dependent on their height in the water column relative to the estuary bed. A similar alteration must be made if turbulence is represented by Kolmogorov microscale eddy sizes.

5.4 SPM RATIO ($SPM_{RATIOEM}$)

To categorise the distribution of particulate matter throughout the macrofloc and microfloc sub-populations, the dimensionless SPM ratio (Manning, 2004b) is used. This was calculated by dividing the percentage of SPM_{macro} by the percentage of SPM_{micro} for each floc population. It must be stressed that this type of computation is unique to instruments such as INSSEV, which can accurately and reliably estimate the floc effective density (by simultaneous size and settling velocity observations) of each individual floc from a respective population. Without this type of measurement, it is not possible to apportion the SPM concentration with any confidence between the microfloc and macrofloc groups. Although this may seem restrictive from an instrumentation perspective, the remainder of this paper will demonstrate how important a knowledge of the distribution of particulate matter is to accurate depositional modelling.

In contrast to the $Ws_{microEM}$, the $SPM_{ratioEM}$ showed a strong dependency solely on SPM concentration (Figure 3c).

$$SPM_{ratioEM} = 0.815 + 0.00318\ SPM - 0.00000014\ SPM^2 \quad R^2 = 0.73 \qquad (17)$$

Low concentrations (10-100 mg l^{-1}) such as ebb conditions during neap tides, tended to create an equally balanced floc population with an $SPM_{ratioEM}$ of approximately unity. Whereas the periods of high entrainment encountered during the more dynamic spring tides, could see the $SPM_{ratioEM}$ rise to between 10-20 for SPM concentrations > 4 g l^{-1}. This corresponds to 91-95.3% of the particulate mass in suspension being contained by macroflocs. This would have a significant effect on the dynamics of a settling floc population and inevitably the depositional flux.

5.5 MASS SETTLING FLUX EMPIRICAL MODEL

Equations 14, 15 and 17 can be combined to form equation 18 from which the total mass settling flux, MSF_{EM} (with the units of $mg.m^{-2}s^{-1}$), can be calculated:

$$MSF_{EM} = \left[\left(1 - \frac{1}{1 + SPM_{ratioEM}}\right) \cdot \left(SPM \cdot Ws_{macroEM}\right)\right] + \left[\frac{1}{1 + SPM_{ratioEM}} \cdot \left(SPM \cdot Ws_{microEM}\right)\right] \qquad (18)$$

This is a very practical way of expressing the inter-relationship between the three core algorithms and can easily be implemented in mathematical simulation models. This type of expression describes the fundamental aspects of estuarine flocs (i.e. their effect on deposition rates) throughout the changing levels of turbulent mixing and particle entrainment, as opposed to a formulation which just has floc settling velocity or size as the dependent variable.

A comparison of the three R^2 fit values indicates that the macrofloc settling velocity is the more consistently predictable parameter, with R^2 values ranging between 0.90-0.99, but the R^2 values of 0.73-0.75 for the remaining two parameters still means that these representations are highly significant for natural empirical data regressed at a confidence level of 95%. To justify the representations described by equations 14, 15 and 17, there must be no direct correlation between τ and SPM concentration. A linear regression of the 157 τ and SPM observations resulted in an R^2 of 0.08, indicating no correlation.

6. Assessment of empirical settling flux model

6.1 INTRODUCTION

In order to quantify the accuracy of the empirical flocculation model (i.e. equation 18), it was tested and compared with a number of existing approaches to floc modelling. Numerical models are used to simulate deposition rates, not settling velocities, so this inter-comparison will be in the form of a prediction of mass settling flux. This requires a MSF value to be calculated for each entire floc spectrum as opposed to just a single group of flocs, therefore approaches that do not use variable settling velocities will assume mean values to represent an entire floc population. Once a modelling approach is formulated and calibrated (where necessary), the only parameters which will be available for each model to calculate a MSF rate will be an input of τ and an SPM concentration value. This is very similar to how a fully 3-D numerical model would utilise a flocculation algorithm, and thus this provides a realistic and equal test of each method's predictive performance. A total of ten methods (denoted by ***M***) were employed in the comparison and a summary is provided in Table 1.

Table 1 Summary of floc parameterisation approaches used during the testing of the new empirical flocculation model (*M1*)

Method number	Description
M1	Full Empirical Flocculation model from this paper (equation 18)
M2	Algorithms which only describe how Ws_{mean} varies with □and SPM. (N.B. These were derived from the INSSEV spectral data sets reported in this paper)
M3	Constant settling velocity, Ws = 0.5 mm s^{-1}
M4	Constant settling velocity, Ws = 1 mm s^{-1}
M5	Constant settling velocity, Ws = 2.5 mm s^{-1}
M6	Constant settling velocity, Ws = 5 mm s^{-1}
M7	Ws_{mean} - SPM concentration power regression relationship
M8	*Lick et al.* [1993] approach
M9	*Van Leussen* [1994] approach
M10	Mean fractal dimension approach

6.2 COMPARISON WITH MEASURED FLUXES

Figure 4 shows the individual MSF values predicted by each of the ten modelling approaches plotted against the corresponding measured MSF rates for each of the 157 cases. It is assumed that flux values measured (i.e. observed) by the INSSEV floc sampling instrument are correct, and strict computational checks were applied to monitor the INSSEV data quality (see Fennessy *et al*, 1997). A statistical assessment was conducted to quantify the deviation of the 157 values calculated by each predictive method, from the 45^{o} ideal fit line plotted on Figures 4a-4j.

A comparison of each pair of individual settling flux values (i.e. predicted and measured) provides only a limited assessment of a model's predictive qualities, as it assumes an equal weighting for each of the 157 observations. However, the complete data set comprised fluxes measured throughout a wide range of estuarine conditions.

Also, when modelling the movement of estuarine sediments throughout consecutive tidal cycles, the precise estimation of the largest fluxes is crucial. Therefore a comparison was made between the measured cumulative total mass settling flux (i.e. the summation of all the 157 individual flux values), which totalled 496286 mg.m^{-2}s^{-1}, and the corresponding cumulative flux totals estimated by each of the ten algorithms. The difference in over or under-prediction by each model, relative to the measured flux total, is expressed as a percentage. All the statistical comparison results are summarised in Table 2. Whilst both the variations in: *i.* the mean error of each individually predicted MSF value, and *ii.* the total MSF, calculated by each modelling method, are also shown graphically as Figures 5 and 6, respectively.

Table 2 Summary of the statistical output from each of the ten approaches mass settling flux predictions in comparison to the observed values. Negative percentage values indicate an under-estimate in the MSF prediction

	Statistical Test	M1	M2	M3	M4	M5	M6	M7	M8	M9	M10
ALL 157 FLOC SAMPLES	Mean Error (%)	-0.8	-13.3	-64.5	-28.9	77.7	255.4	-15.4	-16.2	-15.7	-19.6
	Standard Deviation	10.3	14.9	17.9	35.7	89.4	178.7	34.4	40.0	31.8	179.2
	Variance	105.6	222.4	319.4	1277.6	7984.9	31939.8	1185.7	1597.2	1008.8	32127.1
	Total Cummulative MSF (%)	96.4	78.1	14.1	28.2	70.5	141.0	65.1	57.1	61.6	33.5
	Total Cummulative Error (%)	-124.7	-2094.7	-10120.4	-4540.9	12197.8	40095.6	-2413.2	-2545.1	-2460.2	-3075.4
112 NEAP TIDE FLOC SAMPLES	Mean Error (%)	-0.3	-16.2	-58.1	-16.2	109.6	319.2	-14.0	-12.4	-11.5	-33.6
	Standard Deviation	11.5	21.7	16.2	32.4	81.1	162.1	34.1	39.5	33.4	25.5
	Variance	131.3	470.6	262.9	1051.6	6572.5	26290.2	1160.2	1559.0	1117.2	651.5
	Total Cummulative MSF (%)	96.6	76.0	30.9	61.8	154.5	309.1	74.7	79.2	77.9	57.9
	Total Cummulative Error (%)	-37.8	-1816.3	-6504.7	-1809.4	12276.6	35753.2	-1571.9	-1389.2	-1293.5	-3763.3
45 SPRING TIDE FLOC SAMPLES	Mean Error (%)	-0.3	-16.2	-58.1	-16.2	109.6	319.2	-14.0	-12.4	-11.5	-33.6
	Standard Deviation	11.5	21.7	16.2	32.4	81.1	162.1	34.1	39.5	33.4	25.5
	Variance	131.3	470.6	262.9	1051.6	6572.5	26290.2	1160.2	1559.0	1117.2	651.5
	Total Cummulative MSF (%)	96.6	76.0	30.9	61.8	154.5	309.1	74.7	79.2	77.9	57.9
	Total Cummulative Error (%)	-86.9	-939.9	-3615.8	-2731.5	-78.8	4342.3	-841.3	-1156.0	-1166.7	-2479.3

6.3 RESULTS OF MODEL INTER-COMPARISON

The MSF values calculated by *M1* (equation 18) showed a very close fit to the 45^{o} line throughout the entire range of turbulence and concentration conditions (Figure 4a). Statistically, each individual settling flux estimated by method *M1* was in mean error by only 0.8% (Figure 5a) , at a standard deviation of 10.3% about the mean. This translated into a 96.4% estimation of the cumulative total mass settling flux for all 157 (Figure 6a). The constant settling rates produced a 130% variation in total settling flux, with under predictions of 85% for the slowest velocity (*M3*), through to 41% over predictions for a constant 5 mm s^{-1}. From an initial assessment, methods *M7-M10* seemed to have all performed reasonably well, by producing mean errors ranging between 15-20%. However, the significant amount of scatter around the 45^{o} line (Figures 4g-4j) were reflected in standard deviations 3-4 times greater than those obtained for Method *M1*. Whilst for the mean fractal approach (*M10*) the standard deviation of the mean error was a further 4.5 times larger than those for methods *M7-M9*. In terms of the cumulative total mass settling, the last four approaches only predicted between 34-65% of the flux.

To gain a greater insight into how each model performed during different tidal conditions, comparisons were made by separating the 157 floc data matrix into the neap and spring tidal sub-components. The 112 cases representative of neap tides produced a cumulative total MSF of 28663 $mg.m^{-2}s^{-1}$, and the *M1* (equation 18) estimate was within 3.5% of this total (Figure 6b). Figure 7a shows the scatter of the individual neap tide model predicted flux values relative to the measured fluxes (which are equal to 100%), all plotted against SPM concentration. Method *M1* showed little deviation from the 100% mark, with individual estimates being in error by an average of only 0.3% (Figure 5b).

The low level of suspended concentration, which were typically under 700 mg l^{-1} for neap conditions, resulted in a 22.3% and 20.8% under-estimate in the cumulative total MSF by the SPM power regression (*M7*) and Lick *et al* (1993; *M8*) approaches, respectively. The inclusion of the turbulence parameter as implemented by the van Leussen (1994) method (*M9*) did not fare much better, with a predicted MSF total of 77.9% when compared to the measured value. The very simplified constant settling velocities provided a wide range of errors depending upon the value chosen. The 0.5 mm s^{-1} and 1 mm s^{-1} rates were more representative of what could be classified as typical microfloc settling velocities, and under-predicted the total neaps flux by 69.1% and 38.2%, respectively (Figure 6b). Whereas, the 209.1% over estimate by *M6* (a constant 5 mm s^{-1}) shows that just assigning a faster settling velocity, would produce an even greater misrepresentation of the settling flux. Method *M6* produced individual flux over-predictions of up to 700% (Figure 7a). Generally, the mean error in individual mass flux predictions, and the degree in their dispersion, increased with each faster constant settling velocity increment.

The significant increase in SPM concentration (>700 mg l^{-1}) during spring tide conditions did not affect the accuracy of the MSF prediction of method *M1*, which calculated a cumulative total springs MSF of 449970 $mg.m^{-2}s^{-1}$; this was still only 3.6% less than the measured flux rate (Figure 6c). Apart from method *M6*, which still over predicted by nearly 31%, the remaining methods all under-estimated the cumulative total flux by 34.9-87% (Figure 6c). This was reflected in the greater degree of scatter demonstrated by the individual settling flux under-estimates of methods *M3-M4* and *M7-M10* during the high concentration spring tides (Figure 7b). In terms of their applicability to numerical sediment transport modelling, these excessive over- or under-predictions would minimise or even negate the significant influence of events where flocculation is a major contributor during a tidal cycle, especially within an estuarine turbidity maximum zone.

More details of the floc model intercomparison can be found in Manning and Dyer (2004).

7. Summary and Conclusions

This study has identified the key components which best quantitatively describe a floc population are: the changes in the macrofloc and microfloc settling velocities ($Ws_{macroEM}$ and $Ws_{microEM}$), together with how the suspended matter is distributed in each floc sub-population ($SPM_{ratioEM}$).

The importance of both turbulent shear stress and SPM concentration terms, as independent variables in controlling $Ws_{macroEM}$, was confirmed by a parametric multiple regression statistical analysis of empirical data which produced a highly significant R^2 of 0.91. The $Ws_{macroEM}$ algorithm (equation 14) displays a similar relationship to that proposed by Dyer (1989), with an increase in settling velocity at low shear stresses due to flocculation enhanced by shear, and floc disruption at higher stresses for the same concentration; the transition being a turbulent shear stress of about 0.36 N m^{-2}. This shear threshold corresponds very closely to the value observed during a series of laboratory annular flume experiments by Manning and Dyer (1999).

$Ws_{microEM}$ (equation 15) was very closely correlated with just the τ parameter. Their lack of correlation with SPM concentration probably arises from them being the building blocks from which the larger macroflocs are formed, and the range of sizes possible within the microfloc size fraction is much less than that in the macroflocs. As with the macroflocs, the microfloc settling velocity rose with increasing shear stress until a limiting τ of ~0.42 N m^{-2} was reached. At this point the regression model predicted a peak $Ws_{microEM}$ of ~1 mm s^{-1}; this was significantly slower than the comparative macroflocs. The higher limiting shear stress for the microflocs can be attributed to their stronger inter-connective bondings. Conversely, the $SPM_{ratioEM}$ (equation 17) showed a strong interdependency principally with SPM concentration.

The combination of the three empirical algorithms into a single equation (18) to predict MSF, estimated the total MSF of the 157 measured floc samples from neap and spring tide conditions with a cumulative error of less than 4%. In comparison, the use of single settling velocity values of 0.5 mm s^{-1} and 5 mm s^{-1} were both in error by an average of -86% and +41%, respectively. Representing mean floc settling velocity by: *i)* a simple SPM concentration power-regression relationship, *ii)* the Lick *et al* (1993), and *iii)* the van Leussen (1994) approaches, all under predicted the total cumulative MSF by ~35-43%. Further analysis indicated that methods *M3-M10* all incurred high predictive errors (at times under-estimating by over 70%) as turbidity levels rose in close proximity to the bed. The Ws_{meanEM} (*M2*) proved to be the second most reliable method, although the errors in MSF prediction ranged from cumulative under-estimates of 14-25%.

The findings of this study demonstrate the empirical model (*M1*) has extreme flexibility in adapting to a wide range of estuarine environmental conditions, specifically for applied modelling purposes, by producing reliable mass settling flux predictions in both quiescent waters and the rare occurrence of very turbulent events experienced during extremely high flow velocity conditions where near-bed shear stresses could potentially reach 1-10 N m^{-2}. The *M1* derived mass flux values were also valid for both water columns of very low turbidity and highly saturated benthic suspension layers with SPM concentrations approaching 8.6 g l^{-1}.

Although it is possible to separate the resultant floc characteristics into various inter-related sub-groups, (e.g. macrofloc and microfloc settling velocities), it would be unwise to consider the independent variables of τ and SPM concentration completely separately in any final analysis. The empirical model (*M1*) has shown that it is the simultaneous interaction of turbulent shear stress and concentration which make *in-situ* estuarine floc characteristics intrinsically different from how they would evolve in still water conditions. It is this combined effect which ultimately governs, both spatially and temporally, whether a floc population is composed solely of thousands of high density microflocs or a few hundred higher order, fast settling macroflocs, which are of a much lower effective density.

The reliability and robustness of this empirical model (*M1*) is a testament to the high quality of the data acquisition techniques used. The multiple regression analysis revealed it was possible to accurately gain an insight into the particulate matter distributions, within floc sub-grouping, by using an optically video-based technique that can observe the macroflocs and microflocs which constitute an entire population. In conclusion, empirical studies which do not measure the entire spectral distribution of settling flocs by low intrusive visual interrogation of each floc, risk incorrectly representing the aggregational dynamics which are actually occurring within turbulent water columns.

An algorithm has been devised (see Appendix 1) showing how the newly developed settling flux parameterisation can be implemented in computational sediment transport models.

8. Acknowledgements

The Tamar estuary experimental programme was funded by the EC MAST as part of contract MAS3-CT97-0082 COSINUS (Prediction of cohesive sediment transport and bed dynamics in estuaries and coastal zones with integrated numerical simulation models). The Gironde estuary experiments were funded by the EC TMR SWAMIEE (Sediment and water movement in industrialised estuarine environments) project under contract No. ERBFMRXCT970111. The Dollard estuary experimental programme was funded by the EC MAST project INTRMUD (The Morphological Development of Intertidal Mudflats) under contract MAS3-CT95-0022. The author would like to thank the boat crews and all the technical staff who assisted during all the experiments. The preparation of this report was primarily funded by HR Wallingford (UK), and the Defra / Environment Agency Joint Flood and Coastal Defence Research & Development Programme in Fluvial, Estuarine and Coastal Processes: Estuary Process Research (EstProc) project (under contract No.FD1905/CSA5966). Additional funding by the Natural Environmental Research Council (NERC), contract No.NER/M/S/2002/00108, is also gratefully acknowledged.

9. References

Argaman, Y., and Kaufman, W. J., (1970). "Turbulence and flocculation." J. Sanitary Eng., ASCE, Vol. 96, 223-241.

Bale, A.J. and Morris, A.W., (1987). "In-situ measurement of particle size in estuarine waters." Estuarine, Coastal and Shelf Science, Vol. 24, 253-263.

Burban, P-Y., Lick W. and Lick, J., (1989). "The flocculation of fine-grained sediments in estuarine waters." J. Geophys. Res., Vol. 94 (C6), 8323-8330.

Christie, M.C., Quartley, C.P. and Dyer, K.R., (1997). "The development of the POST system for in-situ intertidal measurements." In Proceedings of the 7th Int. Conf. On Elec. Eng. in Oceanography, Conference Publication No. 439, pp. 39-45, Inst. Elec. Eng., London.

Dyer, K.R., (1989). "Sediment processes in estuaries: future research requirements." J. Geophys. Res., Vol. 94 (C10), 14327-14339.

Dyer, K.R., Bale, A.J., Christie, M.C., Feates, N., Jones, S. and Manning, A.J., (2002). "The turbidity maximum in a mesotidal estuary, the Tamar estuary, UK. Part II: The floc properties." In Fine Sediment Dynamics in the Marine Environment - Proc. in Mar. Sci. Vol. 5., edited by J. C. Winterwerp and C. Kranenburg, pp. 219-232, Elsevier, Amsterdam.

Dyer, K.R., Christie, M.C., Feates, N., Fennessy, M.J., Pejrup, M. and van Der Lee, W., (2000). "An investigation into processes influencing the morphodynamics of an intertidal mudflat, the Dollard estuary, The Netherlands: I. Hydrodynamics and suspended sediment." Estuarine Coastal Shelf Sci., Vol. 50, 607-625.

Eisma, D., (1986). "Flocculation and de-flocculation of suspended matter in estuaries." Neth. J. Sea Res., Vol. 20 (2/3), 183-199.

Eisma, D., Schuhmacher, T., Boekel, H., van Heerwaarden, J., Franken, H., Lann, M., Vaars, A., Eijgenraam, F. and Kalf, J., (1990). "A camera and image analysis system for in-situ observation of flocs in natural waters." Neth. J. Sea Res., Vol. 27, 43-56.

Fennessy, M.J., Dyer, K.R., and Huntley, D.A., (1994). "INSSEV: an instrument to measure the size and settling velocity of flocs in-situ." Marine Geology, Vol. 117, 107-117.

Fennessy, M.J., and Dyer, K.R., (1996). "Floc population characteristics measured with INSSEV during the Elbe estuary intercalibration experiment." Neth. J. Sea Res., Vol. 36 (1-2), 55-62.

Fennessy, M.J., Dyer, K.R., Huntley, D.A. and Bale, A.J., (1997). "Estimation of settling flux spectra in estuaries using INSSEV." In Proceedings of INTERCOH-1994: Cohesive Sediments, edited by N. Burt, R. Parker and J. Watts, pp. 87-104, John Wiley & Son, Chichester, England.

Gibbs, R.J., (1983). "Coagulation rates of clay minerals and natural sediments." J. Sed. Petrol., Vol. 53 (4), 1193-1203.

Gratiot, N. and Manning, A.J., (2004). "An experimental investigation of floc characteristics in a diffusive turbulent flow." In Sediment Transport in European Estuarine Environments, J. Coastal Res. Special Issue, edited by P. Ciavola, M. B. Collins and C. Corbau, Vol. SI 41, (in press).

Heathershaw, A.D., (1979). "The turbulent structure of the bottom boundary layer in a tidal current." Geophys. J. R. astr. Soc., Vol. 58, 395-430.

HR Wallingford, (2002). "Estuary Process Research project (EstProc): Inception Report." Report prepared by the Estuary Process Consortium for the Defra and Environment Agency Joint Flood and Coastal Theme, Report No. FD1905/TR1, 53 pp.

Kineke, G.C., Sternberg, R.W. and Johnson, R., (1989). "A new instrument for measuring settling velocity in-situ." Marine Geology, Vol. 90, 149-158.

Kolmogorov, A.N., (1941a). "The local structure of turbulence in incompressible viscous fluid for very large Reynolds numbers." C. R. Acad. Sci. URSS, Vol. 30, 301 pp.

Kolmogorov, A.N., (1941b). "Dissipation of energy in locally iscotropic turbulence." C. R. Acad. Sci. URSS, Vol. 32, 16 pp.

Krone, R. B., (1963). "A study of rheological properties of estuarial sediments." Report No. 63-68, Hyd. Eng. Lab. and Sanitary Eng. Lab., University of California, Berkeley.

Kranenburg, C., (1994). "The fractal structure of cohesive sediment aggregates." Estuarine Coastal Shelf Sci., Vol. 39, 451-460.

Lick, W., (1994). "Modelling the transport of sediment and hydrophobic contaminants in surface waters." in Proc. U.S.A. / Israel Workshop on monitoring and modelling water quality, (Haifa, Israel).

Lick, W., Huang, H. and Jepsen, R., (1993). "Flocculation of fine-grained sediments due to differential settling." J. Geophys. Res., Vol. 98 (C6), 10279-10288.

Manning, A.J., (2001). "A study of the effect of turbulence on the properties of flocculated mud." Ph.D. Thesis, Institute of Marine Studies, University of Plymouth, UK, 282 pp.

Manning, A.J., (2004a). "The effects of turbulence on estuarine flocculation." In Sediment Transport in European Estuarine Environments, J. Coastal Res. Special Issue, edited by P. Ciavola, M. B. Collins and C. Corbau, Vol. SI 41, (in press).

Manning, A.J., (2004b). "Observations of the properties of flocculated cohesive sediment in three western European estuaries." In Sediment Transport in European Estuarine Environments, J. Coastal Res. Special Issue, edited by P. Ciavola, M. B. Collins and C. Corbau, Vol. SI 41, (in press).

Manning, A.J., and Dyer, K.R., (1999). "A laboratory examination of floc characteristics with regard to turbulent shearing." Marine Geology, Vol. 160, 147-170.

Manning, A.J. and Dyer, K.R., (2002a). "A comparison of floc properties observed during neap and spring tidal conditions." In Fine Sediment Dynamics in the Marine

Environment - Proc. in Mar. Sci. Vol. 5., edited by J. C. Winterwerp and C. Kranenburg, pp. 233-250, Elsevier, Amsterdam.

Manning, A.J. and Dyer, K.R., (2002b). “The use of optics for the in-situ determination of flocculated mud characteristics.” Journal of Optics A: Pure and Applied Optics, Institute of Physics Publishing, Vol. 4, S71-S81.

Manning, A.J. and Dyer, K.R., (2004). “Mass settling flux of fine sediments: measurements and predictions.” Journal of Geophysical Research, (sub judice).

Manning, A.J., Dyer, K.R., Lafite, R. and Mikes, D., (2004). “Flocculation measured by video based instruments in the Gironde estuary during the European Commission SWAMIEE Project.” In Sediment Transport in European Estuarine Environments, J. Coastal Res. Special Issue, edited by P. Ciavola, M. B. Collins and C. Corbau, Vol. SI 41, (in press).

McCave, I.N., (1984). “Erosion, transport and deposition of fine-grained marine sediments.” In: Fine-Grained Sediments: Deep Water Processes and Facies, edited by D.A.V Stow and DJ.W. Piper, pp. 35-69.

McCave, I.N. and Gross, T.F., (1991). “In-situ measurements of particle settling velocity in the deep sea.” Marine Geology, Vol. 99, 403-411.

Nakagawa, H., and Nezu, I., (1975). “Turbulence in open channel flow over smooth and rough beds.” Proc. Japan Soc. Civ. Eng., Vol. 241, 155-168.

Owen, M.W., (1976). “Determination of the settling velocities of cohesive muds.” HR Wallingford Report No. IT 161, 8 pp.

Soulsby, R.L., (1983). “The bottom boundary layer of shelf seas.” In Physical oceanography of coastal and shelf seas, edited by B. Johns, pp. 189-266, Elsevier, New York.

Spinrad, R.W., Bartz, R. and Kitchen, J.C., (1989). “In-situ measurements of marine particle settling velocity and size distributions using the remote optical settling tube.” J. Geophys. Res., Vol. 94 (C1), 931-938.

Stolzenbach, K.D. and Elimelich, M., (1994). “The effect of density on collisions between sinking particles: implications for particle aggregation in the ocean.” J. Deep-Sea Res., Vol. 41 (3), 469-483.

Ten Brinke, W.B.M., (1994). “Settling velocities of mud aggregates in the Oosterschelde Tidal basin (The Netherlands) determined by a submersible video system.” Estuarine, Coastal and Shelf Science, Vol. 39, 549-564.

Van Leussen, W., (1988). “Aggregation of particles, settling velocity of mud flocs: A review.” in Physical Processes in Estuaries, edited by J. Dronkers and W. van Leussen, pp. 347-403, Springer-Verlag, Berlin.

Van Leussen, W., (1994). “Estuarine macroflocs and their role in fine-grained sediment transport.” Ph.D. Thesis, University of Utrecht, The Netherlands, 488 pp.

Winterwerp, J.C., (1998). "A simple model for turbulence induced flocculation of cohesive sediment." J. Hyd. Eng., Vol. 36 (3), 309-326.

Winterwerp J. C., (1999). "On the dynamics of high-concentrated mud suspensions." Ph.D. Thesis, Delft University of Technology, Faculty of Civil Engineering and Geosciences, The Netherlands, 172 pp.

Figures

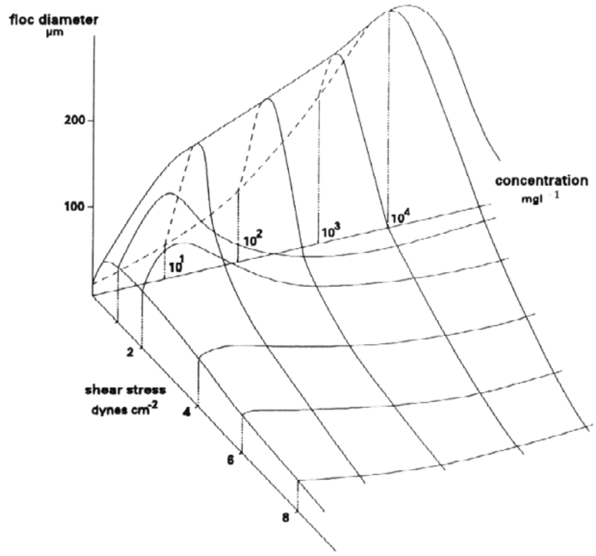

Figure 1 Conceptual diagram showing the relationship between floc modal diameter, suspended sediment concentration and shear stress (Dyer, 1989)

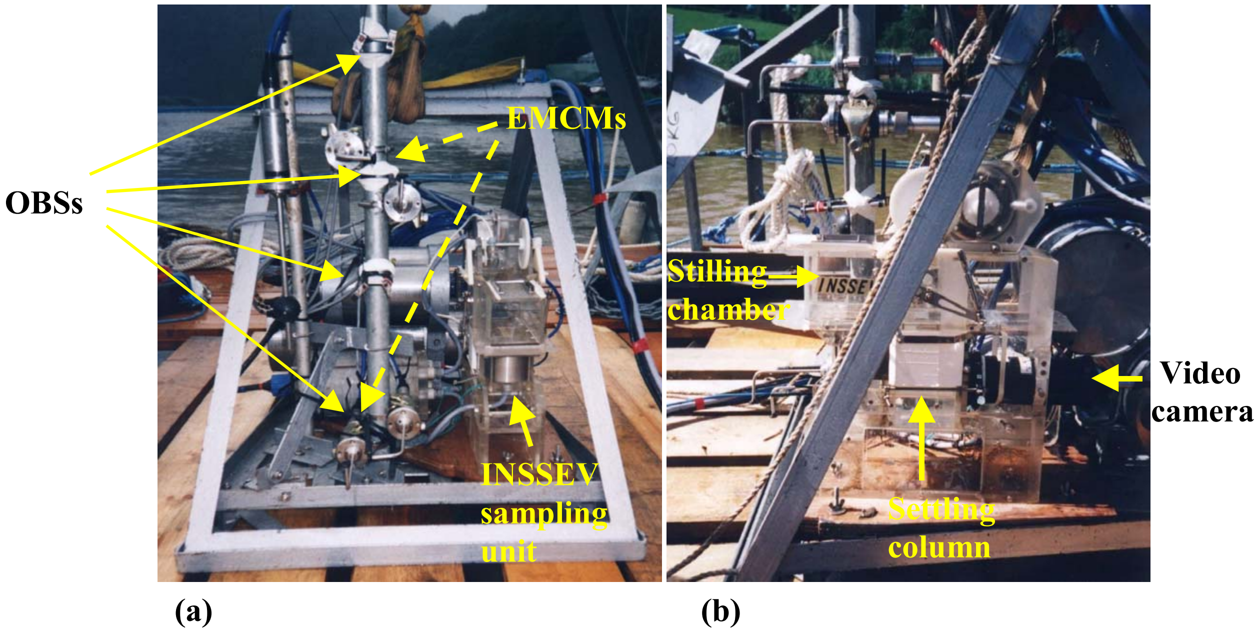

Figure 2 INSSEV and POST sensors mounted on the estuarine bed frame – (*a*) front view and (*b*) side view

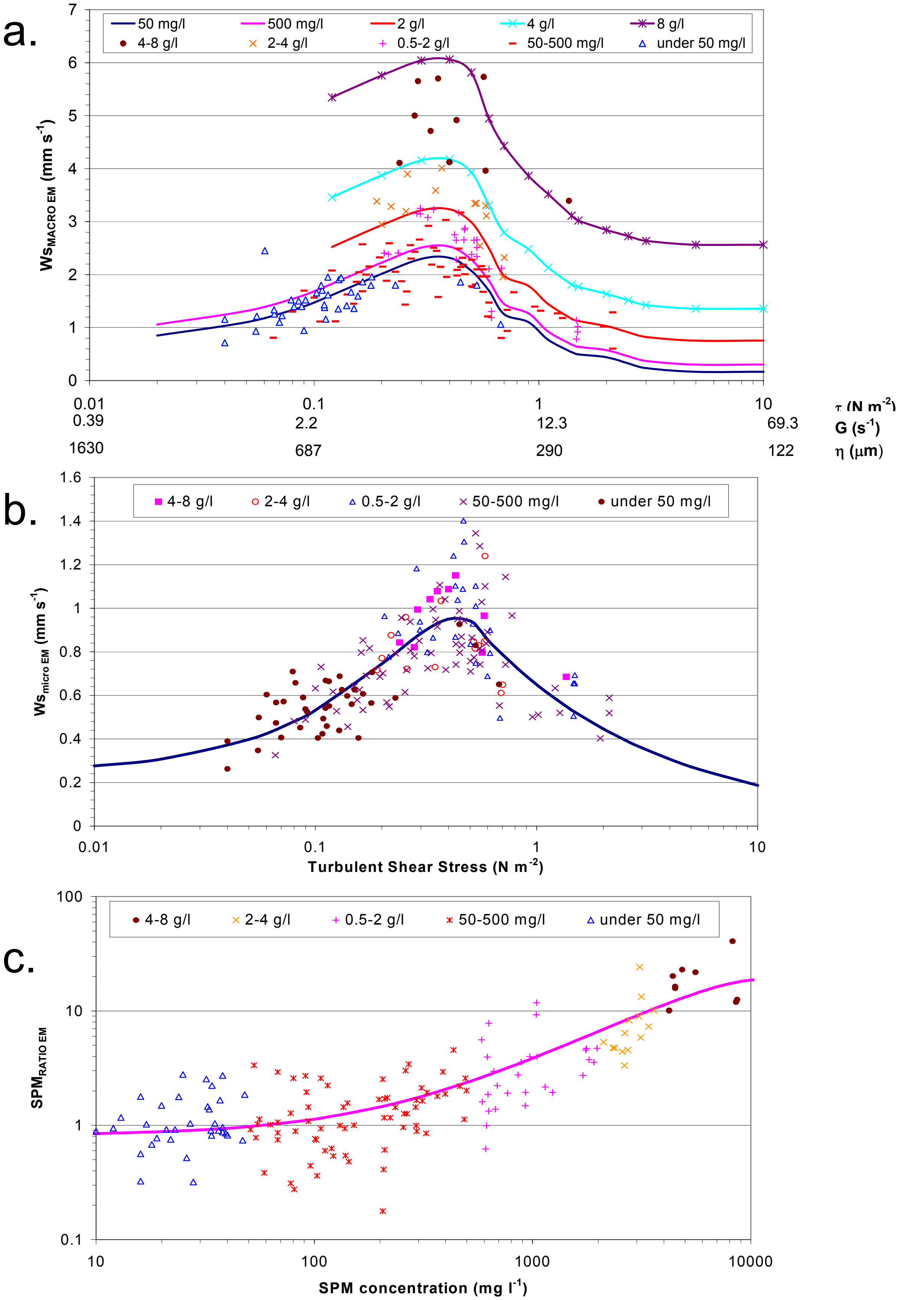

Figure 3 Representative plots of the statistically generated regression curves, together with the experimental data points, illustrating the three contributing components for the empirical flocculation model: *a*) Wsmacro EM (eqn 14), *b*) Wsmicro EM (eqn 15) and *c*) SPMratio EM (eqn 17)

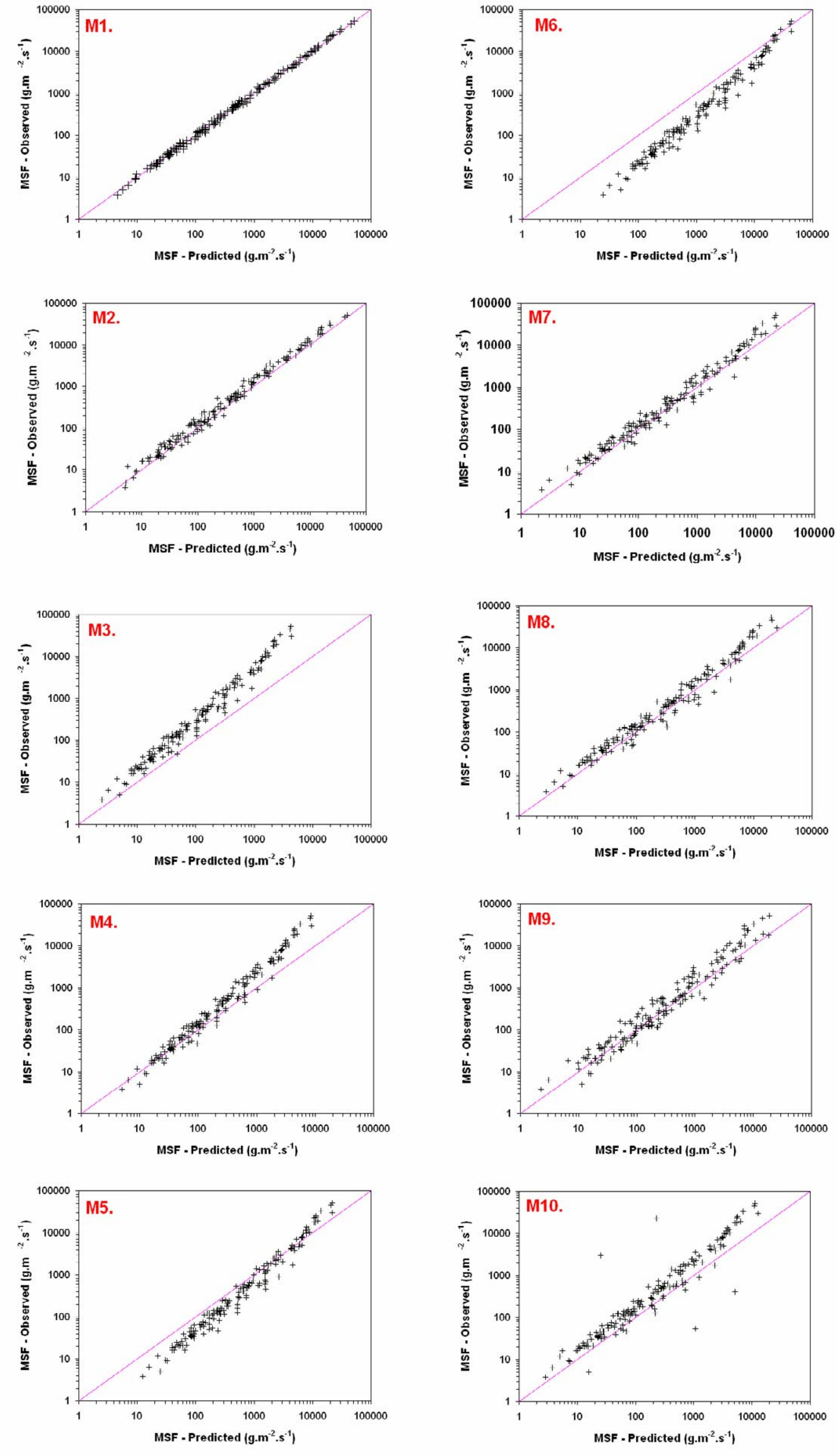

Figure 4 The 157 individual mass settling flux (MSF) observations plotted against the corresponding 157 MSF values as predicted by each floc model approach (*M1-M10)*

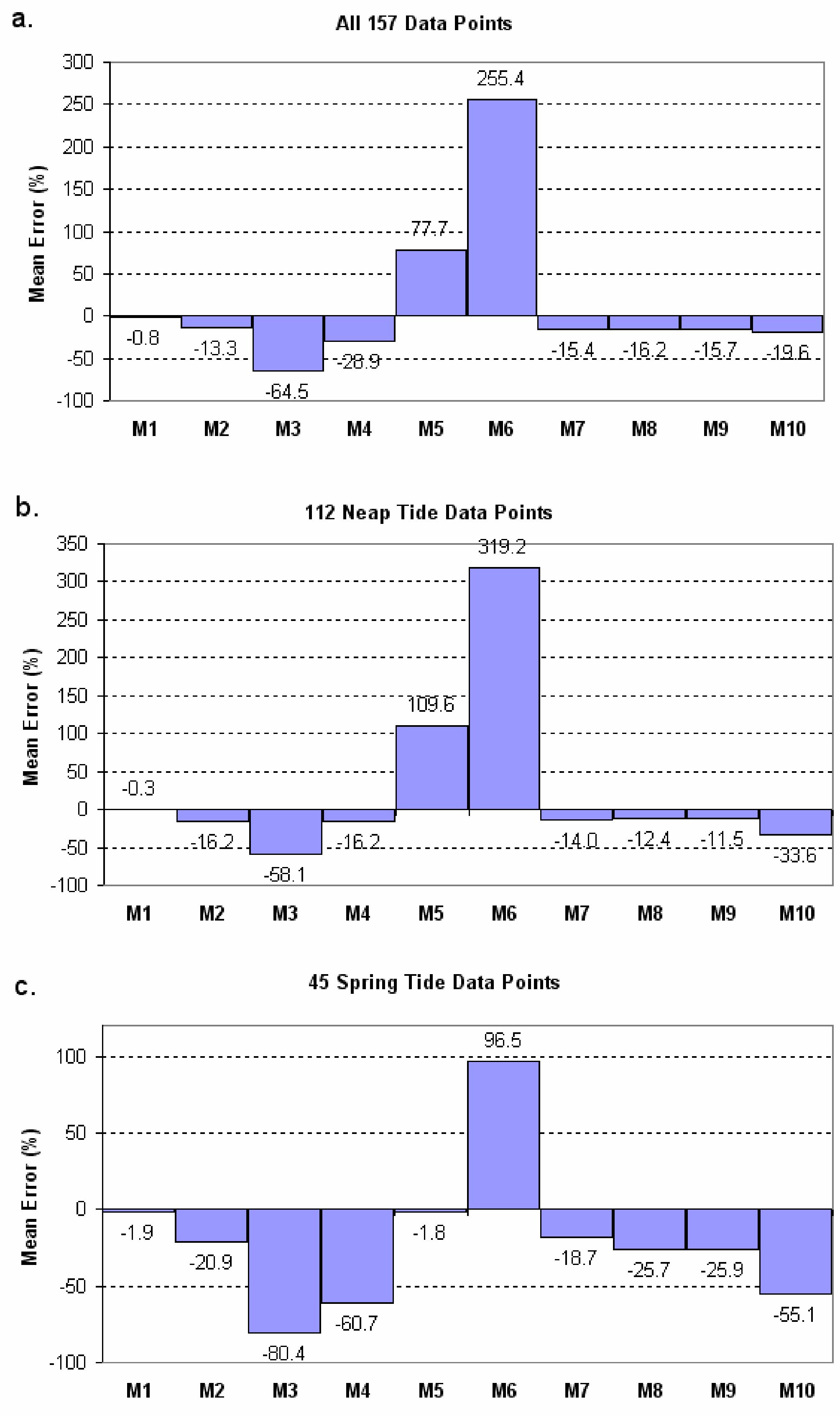

Figure 5 The mean error (expressed as a %) demonstrated by each of the individual MSF values as calculated by each modelling method, for: *a.* all 157 flux values, *b.* Neap tides (112 flux values), and *c.* Spring tides (45 flux values). Negative values indicate overall errors which are under-predictions in MSF.

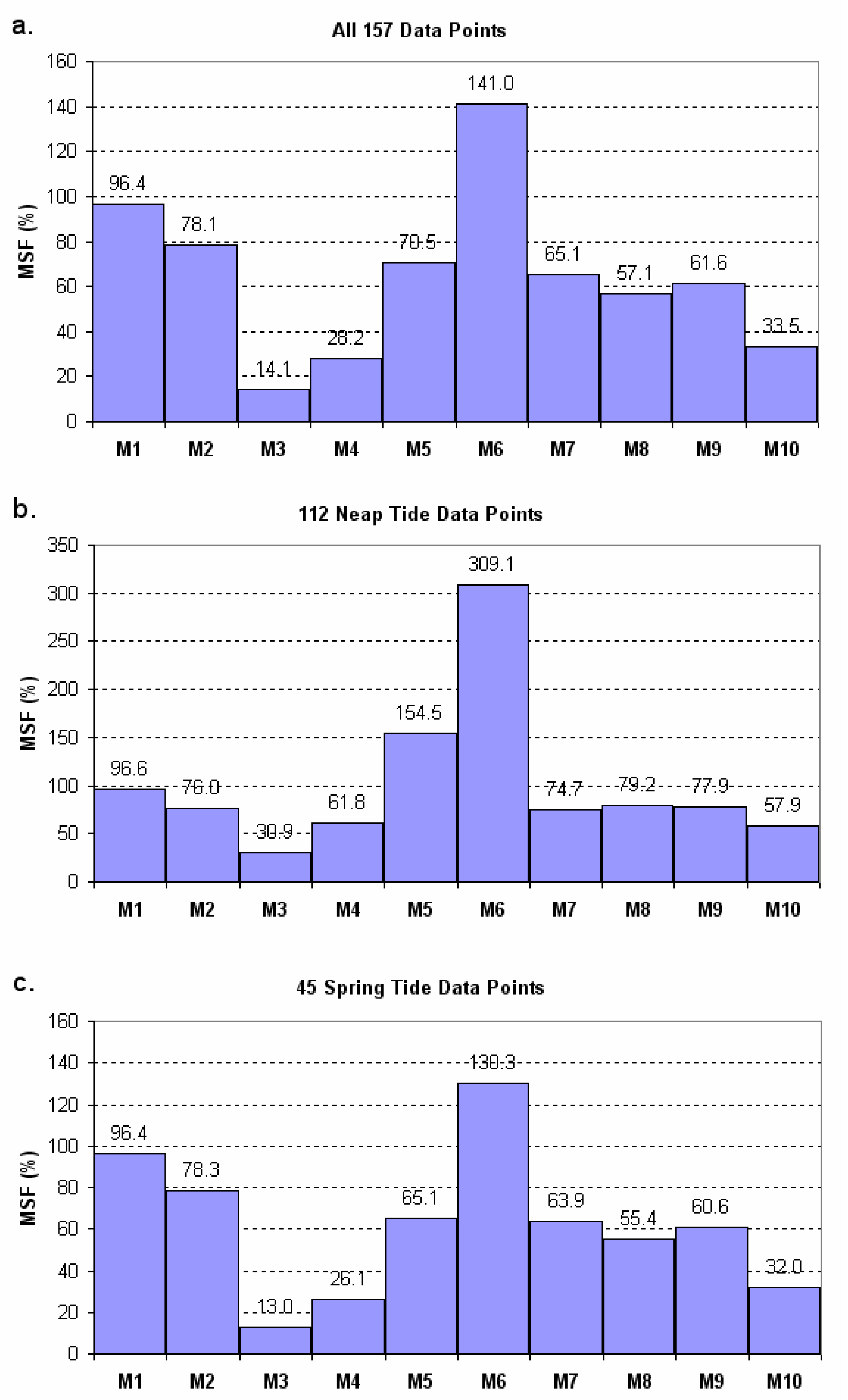

Figure 6 The cummulative total mass settling flux (MSF) expressed as a percentage, as calculated by each modelling method, for: ***a.*** all 157 flux values, ***b.*** Neap tides (112 flux values), and ***c.*** Spring tides (45 flux values). 100% = the total MSF observed

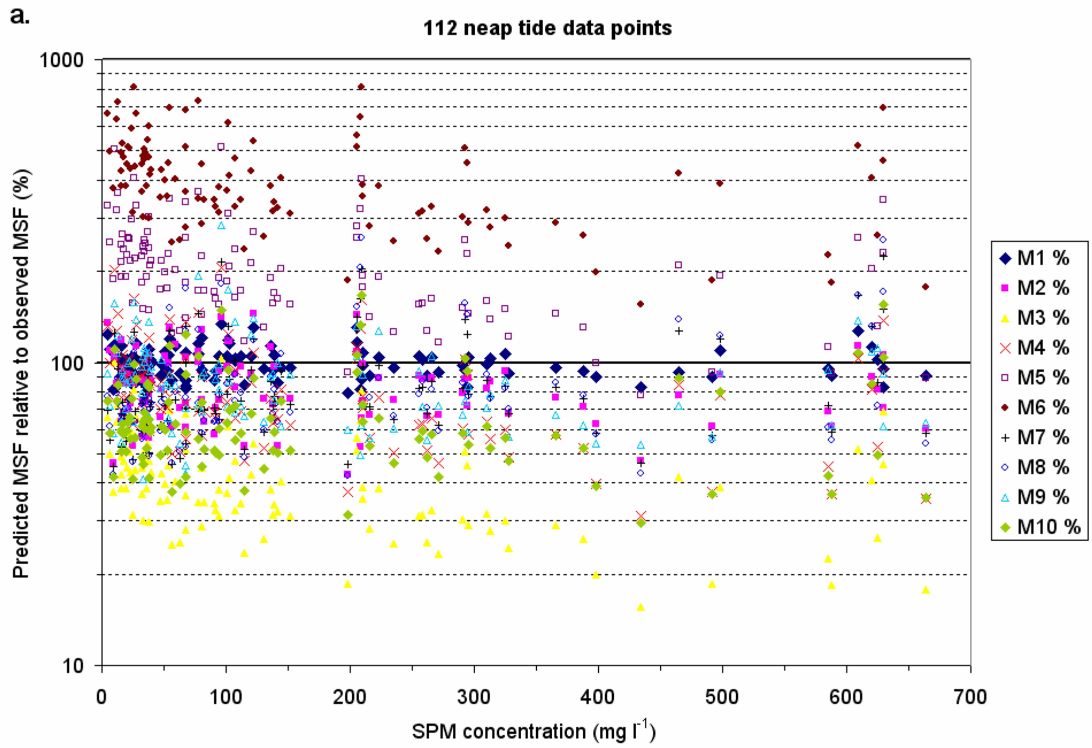

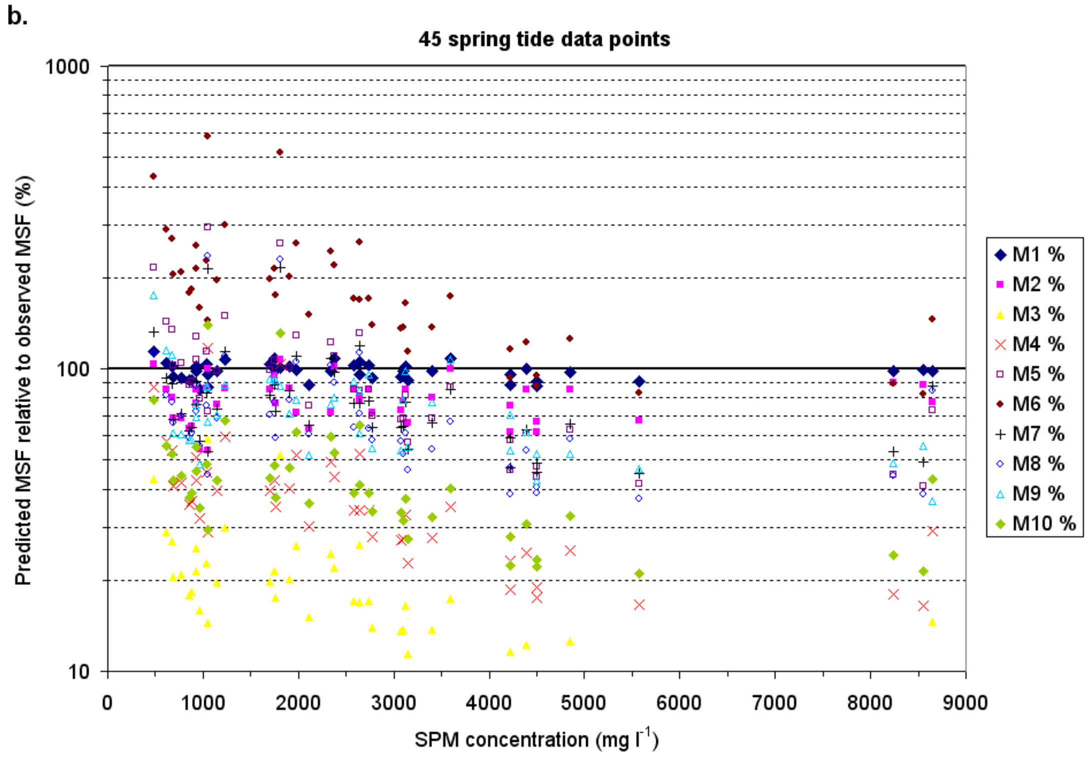

Figure 7 Individual mass settling flux (MSF) values, as predicted by each floc model approach (*M1-M10*) plotted against SPM concentration; for (*a*) 112 neap tide data points and (*b*) 45 spring tide data points. Each corresponding observed flux value is equal to 100%

Appendix

Appendix 1 Method Algorithm

Aim To calculate the mass settling flux of flocculated cohesive sediment in a turbulent estuarine water column.

Scientific background

For predicting the transport and fate of sediment movement in estuaries, the determination of the various spatial and temporal mass fluxes is essential. One area which has caused numerous problems, is the modelling and parameterised description of the vertical mass settling flux of fine cohesive sediment, which becomes the depositional flux close to slack water. This flux is the product of the suspended particulate matter (SPM) concentration and the settling velocity. For non-cohesive sediment this is a relatively simple process as the settling velocity is proportional to the particle size. Whereas estuarine muds, which are composed of combinations of clay minerals and different types of biological matter, have the potential to flocculate in to larger, low density aggregates called flocs.

Turbulent shear generated in estuarine water columns is recognised as having a controlling influence on both the formation of mud flocs, and their break-up (Manning, 2004a). However, to date there have been no *in-situ* studies which have quantified the flocculation process with the specific emphasis of taking floc effective density, and consequently particulate mass distribution variations, into account, within both continually changing estuarine suspended concentration gradients and varying intensities of turbulent mixing. This is mainly due to the fragility of the fastest settling macroflocs, which are easily broken-up upon sampling.

The new flocculation model, developed as part of the EstProc project, is based entirely on empirical observations made using low intrusive floc and turbulence data acquisition techniques, from a wide range of estuarine water column conditions. In particular, the floc population size and settling velocity spectra were sampled using the unique video-based INSSEV: *IN-Situ* SEttling Velocity instrument, which was developed at the University of Plymouth. This provided a total of 157 floc data sets, from experiments conducted within the framework of three recent European Commission funded projects: COSINUS, SWAMIEE and INTRMUD (see Manning, 2004b).

The algorithms were generated by a parametric multiple regression statistical analysis of key parameters which were generated from the raw spectral data (detailed derivations and testing of the algorithms are described in: Manning, 2004c; Manning and Dyer, 2004). The multi-regression identified the key components which best quantitatively describe a floc population as being: the changes in the macrofloc (flocs size > 160 μm) and microfloc (flocs size < 160 μm) settling velocities ($Ws_{macroEM}$ and $Ws_{microEM}$), together with how the suspended matter is distributed across each floc sub-population ($SPM_{ratioEM}$).

Improvement in understanding

The new method improves on existing methods because:

- The algorithm is based on a multiple regression analysis of 157 uniquely comprehensive empirical flocculation and turbulence data sets, which were acquired from three different estuarine field experiments and two laboratory studies.

- The algorithm can estimate the settling velocity of both the macrofloc and microfloc sub-populations, in response to changes in turbulence and SPM concentration at an individual temporal and spatial point in an estuarine water column simulation. This method can also apportion the concentration distribution between the macrofloc and microfloc fractions, and correlate this floc mass to the respective settling velocities of each fraction.
- Typically these algorithms only require the input of two variables (turbulent shear stress and SPM concentration), which simplifies their inclusion in numerical simulation sediment transport models, and reduces computer processing time.
- The flocculation algorithm has extreme flexibility in adapting to a wide range of estuarine environmental conditions, specifically for applied modelling purposes, by producing reliable mass settling flux predictions in both quiescent waters, and on the rare occurrence of very turbulent events experienced during extremely high flow velocity conditions, where near-bed shear stresses could potentially reach the order of 1-10 N m^{-2}. The derived mass flux values are also valid for both water columns of very low turbidity and highly saturated benthic suspension layers with concentration approaching 8.6 g l^{-1}.
- It has been tested against independently acquired *in-situ* data sets, and gives good agreement.

Implementation

The algorithm is written in a step-by-step "recipe" style, which can easily be coded for numerical computer applications. The complete algorithm will calculate mass settling flux, or the three main components (equations *A1*, *A2* and *A4*) can be used in a stand-alone mode if required.

Algorithm

Inputs

The algorithm requires three-dimensional grid (node) data inputs of the following parameters:

Turbulent shear stress (N m^{-2})	τ
Suspended particulate matter concentration (mg l^{-1})	SPM
Root mean square of the gradient in turbulent velocity fluctuations (s^{-1})	G
Von Karman constant (no units)	κ
Kinematic viscosity (m^2 s^{-1})	ν
Water density (kg m^{-3})	ρ_w
Distance above the estuary bed (m)	z

Outputs

The algorithm can calculate the following outputs for each point (node) on a predetermined three-dimensional numerical model grid:

Macrofloc settling velocity (mm s^{-1})	Ws_{macroEM}
Microfloc settling velocity (mm s^{-1})	$Ws_{microEM}$
Suspended particulate matter ratio (no units)	$SPM_{ratioEM}$
Total mass settling flux (mg.m^{-2} s^{-1})	MSF_{EM}

Calculate macrofloc settling velocity
For τ ranging between 0.04-0.7 N m^{-2}:

$$Ws_{macroEM} = 0.644 + 0.000471\ SPM + 9.36\ \tau - 13.1\ \tau^2 \qquad (A1a)$$

For τ ranging between 0.6-1.5 N m^{-2}:
$$Ws_{macroEM} = 3.96 + 0.000346\ SPM - 4.38\ \tau + 1.33\ \tau^2 \qquad (A1b)$$

For τ ranging between 1.4-5 N m^{-2}:
$$Ws_{macroEM} = 1.18 + 0.000302\ SPM - 0.491\ \tau + 0.057\ \tau^2 \qquad (A1c)$$

- Continuity between each relationship can be achieved by calculating a $Ws_{macroEM}$ value using both adjacent equations (at a specific τ) and obtaining a single transitional $Ws_{macroEM}$ value from linear interpolation.
- The transition shear stress zone between eqns *A1a-A1b* is 0.6-0.7 N m^{-2}.
- The transition shear stress zone between eqns *A1b-A1c* is 1.4-1.5 N m^{-2}.

Calculate the microfloc settling velocity
For τ ranging between 0.04-0.55 N m^{-2}:

$$Ws_{microEM} = 0.244 + 3.25\ \tau - 3.71\ \tau^2 \qquad (A2a)$$

For τ ranging between 0.51-10 N m^{-2}:
$$Ws_{microEM} = 0.65\ \tau^{-0.541} \qquad (A2b)$$

- Continuity between each relationship can be achieved by calculating a $Ws_{microEM}$ value using both adjacent equations (at a specific τ) and obtaining a single transitional $Ws_{microEM}$ value from linear interpolation.
- The transition shear stress zone occurs between a τ of 0.51-0.55 N m^{-2}.

Calculate an alternative turbulence parameter format (optional)
If both equations *A1* and *A2* are to be incorporated into the framework of a numerical model where the turbulence input parameter is of the turbulent shear G format, all the τ functions must be replaced with the following τ_{mod} equation:

$$\tau_{mod} = \rho_w\ [(G^2\ .\ \kappa\ .\ \nu\ .\ z)^{1/3}]^2 \qquad (A3)$$

This is because unlike the τ parameter, corresponding values of G are dependent on their height in the water column relative to the estuary bed.

Calculate the suspended particulate matter ratio
$$SPM_{ratioEM} = 0.815 + 0.00318\ SPM - 0.00000014\ SPM^2 \qquad (A4)$$

Calculate the total mass settling flux
$$MSF_{EM} = \left[\left(1 - \frac{1}{1 + SPM_{ratioEM}}\right) \cdot (SPM \cdot Ws_{macroEM})\right] + \left[\frac{1}{1 + SPM_{ratioEM}} \cdot (SPM \cdot Ws_{microEM})\right] \qquad (A5)$$

Limits of applicability

The algorithm is applicable where there is high resolution, fully three dimensional coverage of SPM concentration and turbulent shear stress; either as an empirical data set or values generated by a numerical model.

No multiple regression data points were available for SPM concentrations over 1 g l^{-1} when the turbulent shear stress fell below 0.1 N m^{-2}, and therefore this should be regarded as a further boundary limit to equation *A1a*.

Validation

The algorithms were tested against data acquired from a series of field experiments funded by the Natural Environmental Research Council which were conducted in the upper reaches of the Tamar estuary (UK), and placed the measurements within the tidal trajectory of the turbidity maximum. For spring tide measurements made on the 15th April 2003, a concentrated benthic suspension layer formed in close proximity to the bed on the ebb producing a peak concentration of 4.2 g l^{-1}. Turbulent shear stresses for the tidal cycle ranged from 0.04-1.6 N m^{-2}. The algorithms calculated the cumulative total mass settling flux for the entire 12.5 hour tidal cycle to within 93% of the measured flux.

It is anticipated that the algorithms will be tested within an HR Wallingford TELEMAC-3D numerical model of a cross-section of the Thames estuary. If this test is successful, it will be followed by testing the algorithms in a 3D beach cross-section.

References

Manning, A.J., (2004a). The observed effects of turbulence on estuarine flocculation. In: P. Ciavola, M. B. Collins and C. Corbau (eds), Sediment Transport in European Estuaries, Journal of Coastal Research Special Issue, SI 41, (in press).

Manning, A.J., (2004b). Observations of the properties of flocculated cohesive sediment in three western European estuaries. In: P. Ciavola, M. B. Collins and C. Corbau (eds), Sediment Transport in European Estuaries, Journal of Coastal Research Special Issue, SI 41, (in press).

Manning, A.J., (2004c). The development of new algorithms to parameterise the mass settling flux of flocculated estuarine sediments, HR Wallingford Technical Report No. TR 145, 26 pp.

Manning, A.J. and Dyer, K.R., (2004). Mass settling flux of fine sediments: measurements and predictions. Journal of Geophysical Research, (sub judice).